ISSN 0021-3640, JETP Letters, 2020, Vol. 111, No. 5, pp. 286–292. © Pleiades Publishing, Inc., 2020.
Russian Text © The Author(s), 2020, published in Pis'ma v Zhurnal Eksperimental'noi i Teoreticheskoi Fiziki, 2020, Vol. 111, No. 5, pp. 321–327.

CONDENSED MATTER

Collapse of the Fano Resonance Caused by the Nonlocality of the Majorana State

S. V. Aksenov[a, *] and M. Yu. Kagan[b, c, **]

[a] *Kirensky Institute of Physics, Federal Research Center KSC, Siberian Branch, Russian Academy of Sciences, Krasnoyarsk, 660036 Russia*

[b] *National Research University Higher School of Economics, Moscow, 101000 Russia*

[c] *Kapitza Institute for Physical Problems, Russian Academy of Sciences, Moscow, 119334 Russia*

**e-mail: asv86@iph.krasn.ru*

***e-mail: kagan@kapitza.ras.ru*

Received January 14, 2020; revised February 10, 2020; accepted February 10, 2020

Owing to the nonlocal character of the Majorana state, the corresponding excitations are of great interest. It is demonstrated that the direct consequence of such nonlocality is the collapse of the Fano resonance manifesting itself in the conductance of an asymmetric interference device, the arms of which are connected by a one-dimensional topological superconductor. In the framework of the spinless model, it is shown that the predicted effect is associated with an increase in the multiplicity of the degeneracy of the zero-energy state of the structure arising at the critical point of the Kitaev model. Such an increase leads to the formation of a bound state in the continuum.

DOI: 10.1134/S0021364020050057

1. The formation of bound states in the continuum (BSCs) in quantum systems is a particular case of coupling between continuous and discrete states, when their hybridization vanishes [1, 2]. Bound states in the continuum can be due both to fundamental mechanisms related to a certain symmetry of the structure [3] and to an accidental vanishing of the mentioned coupling occurring in the course of continuous change in the parameters of the system [4]. In the ideal case, systems with BSCs should exhibit infinite Q factors, which makes them quite promising for optical applications, such as lasers, filters, and detectors [5].

Quantum dot arrays are popular objects often exhibiting BSCs [6]. This is already evident in the simplest case of two dots whose eigenstates can be considered as bonding and antibonding ones. Then, breaking the symmetry of an open system by the continuous variation of the parameters characterizing the tunnel coupling of the double quantum dot with contacts, we can trace the crossover from the situation where the antibonding state is a BSC at the symmetric parallel connection to that where both of these states have the same finite lifetime at the serial connection [7].

In the intermediate case of an asymmetric parallel connection, the conductance resonance related to the antibonding state has the form of a Fano resonance [8], the width of which is proportional to the value of hybridization of this state with the continuum. A similar picture is observed when the Aharonov–Bohm phase is taken into account [9, 10]. As a result, in highly asymmetric transport geometry, the conductance is characterized by the presence of a wide Breit–Wigner resonance and a narrow Fano resonance, similar to the Dicke effect in optics [11]. Thus, the Fano resonance can be interpreted as a precursor of a BSC, and its collapse is a point in the parametric space where the BSC appears [12, 13]. An increase in the number of quantum dots in the structure leads to the corresponding increase in the number of BSCs [14]. Many-particle effects also lead to the formation of additional BSCs and Fano resonances [15, 16]. In turn, the spin–orbit coupling and Zeeman splitting make it possible to implement the spin filtering effect based on these features [17, 18]. Note that BSCs arise in the systems under discussion naturally because these systems are not one-dimensional in the coordinate or energy space [19, 20].

The phenomenon of topological superconductivity is of great interest since it is promising mainly for quantum computations, which are resistant to the processes disturbing the phase of a qubit state. One of the scenarios allowing the actual formation of the Majorana state (MS) in one-dimensional systems is the combination of spin–orbit coupling, superconducting pairing, and magnetic field [21–23]. In this case, at a certain relation between the parameters characterizing the normal phase, an odd number of Fermi points arise at $k \geq 0$ (k is the wave vector). As a result, the

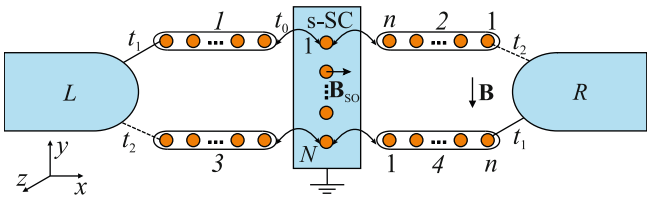

Fig. 1. (Color online) Aharonov–Bohm ring with the arms connected by the superconducting wire exhibiting the Rashba spin–orbit coupling.

superconducting pairing of electrons belonging to one subband, i.e., the effective *p*-wave pairing, takes place. Thus, a wire becomes equivalent to a Kitaev chain, which is an idealized one-dimensional system, where the formation of the MS was demonstrated for the first time [24]. Spin–orbit coupling is important also because the self-conjugated operator of the quasiparticle excitation with zero energy cannot have the form $\beta = ua_\uparrow + va_\downarrow^+$. Several tunneling spectroscopy experiments with InAs and InSb superconducting wires (SWs) exhibiting the strong spin–orbit coupling and induced superconducting pairing provide evidence in favor of the MS formation in the aforementioned structures [25].

However, despite the progress in epitaxial growth techniques and measurement methods [26], the quantization of the conductance obtained at zero voltage does not provide sufficient evidence for the formation of a topologically nontrivial phase in the structures under discussion [27]. As a result, the search for alternative ways of detecting the MS [28], in particular, using the nonlocal nature of this excitation, is a topical task. In [29], the transport characteristics of the symmetric Aharonov–Bohm ring, the arms of which are connected by a SW bridge (see Fig. 1 at $t_1 = t_2$), are analyzed. It is shown that the conductance exhibits the Dicke effect if the nontrivial phase arises in the wire. Moreover, the properties of the Fano resonance depend on the overlap of the Majorana wavefunctions localized at opposite ends of the SW.

In this work, we study the asymmetric ring shown in Fig. 1, where asymmetry corresponds to different tunneling parameters between the contacts and device, $t_1 \neq t_2$. It is shown that, in contrast to the previously studied symmetric geometry [29], new Fano resonances appear in the conductance of an asymmetric device. It is found that their width is proportional to the degree of nonlocality of the state of the SW with the lowest energy. In other words, the higher the near-edge probability density, the narrower the Fano resonance. As a result, in the limiting case of two noninteracting Majorana fermions, this conductance feature disappears.

2. The quantum transport features discussed below are due to the SW. The Hamiltonian of the SW has the form

$$\hat{H}_\mathrm{W} = \sum_{j=1}^{N}\left[\sum_\sigma \xi a_{j\sigma}^+ a_{j\sigma} + \left(\Delta a_{j\uparrow}^+ a_{j\downarrow}^+ + iha_{j\uparrow}^+ a_{j\downarrow} + \mathrm{H.c.}\right)\right] + \frac{1}{2}\sum_{\sigma;j=1}^{N-1}\left[-ta_{j\sigma}^+ a_{j+1,\sigma} + i\alpha\sigma a_{j\bar{\sigma}}^+ a_{j+1,\sigma} + \mathrm{H.c.}\right]. \quad (1)$$

Here, $\xi = \epsilon_d - \mu$ is the on-site energy, where ϵ_d is the energy of the gate electric field and μ is the chemical potential; t is the hopping integral for the nearest sites; α is the Rashba spin–orbit coupling constant; Δ is the *s*-wave superconducting pairing parameter; and h is the Zeeman energy related to the magnetic field $\mathbf{B}$ in the device plane. Then, the topologically nontrivial phase takes place if the following inequalities are valid [21, 22]:

$$(\xi - t)^2 + \Delta^2 < h^2 < (\xi + t)^2 + \Delta^2. \quad (2)$$

Note that, although α formally does not appear in inequalities (2), a nonzero spin–orbit coupling is essential for the formation of the MS, as was already mentioned in Section 1. Moreover, the effective Rashba field $\mathbf{B}_{SO}$ should be perpendicular to the Zeeman field $\mathbf{B}$. Further on, in our calculations, all energy parameters are measured in units of t: $t = 1$, $\Delta = 0.25$, $\alpha = 0.2$, and $\mu = 0$.

The wires in the normal phase (NW), which are the arms of the ring (see Fig. 1), are assumed identical. Their Hamiltonians $\hat{H}_{1-4}$ are obtained from Eq. (1) at $\Delta = \alpha = 0$. The coupling between the SW and NWs is described by the tunneling Hamiltonian

$$\hat{H}_\mathrm{T} = -t_0\sum_\sigma\left[\left(b_{Ln\sigma}^+ + b_{Rn\sigma}^+\right)a_{1\sigma} + \left(d_{L1\sigma}^+ + d_{R1\sigma}^+\right)a_{N\sigma}\right] + \mathrm{H.c.}, \quad (3)$$

where t_0 is the hopping integral between the edge SW and NW sites, $b_{\mathrm{L(R)}n\sigma}^+$ is the creation operator for an electron with the spin projection σ at the last site in the left (right) upper NW, and $d_{\mathrm{L(R)}1\sigma}^+$ is the creation operator for an electron with the spin projection σ at the first site in the left (right) lower NW. In turn, the coupling between the device (SW + NW) and contacts is also described by the tunneling Hamiltonian, which at the same time plays the role of the interaction operator in the diagram technique for nonequilibrium Green's functions

$$\hat{V} = -\sum_{k\sigma}\left[c_{\mathrm{L}k\sigma}^+\left(t_1 b_{\mathrm{L}1\sigma} + t_2 d_{\mathrm{L}n\sigma}\right) + c_{\mathrm{R}k\sigma}^+\left(t_2 b_{\mathrm{R}1\sigma} + t_1 d_{\mathrm{R}n\sigma}\right)\right] + \mathrm{H.c.}, \quad (4)$$

where $c_{\mathrm{L(R)}k\sigma}^+$ is the creation operator for an electron with the wave vector k and the spin projection σ at the

left (right) contact and $t_{1,2}$ are the hopping integrals between the contacts and device. The Hamiltonian for the ith contact (i = L or R) has the simple form $\hat{H}_i = \sum_k (\epsilon_k - \mu_i) c^+_{ik\sigma} c_{ik\sigma}$, where $\mu_{L,R} = \mu \pm eV/2$ is the electrochemical potential of the contact including the applied bias voltage.

To calculate the steady-state current flowing across the device, it is convenient to diagonalize its Hamiltonian, $\hat{H}_D = \hat{H}_W + \sum_{i=1}^{4} \hat{H}_i + \hat{H}_T$, using the Nambu operators in the site representation, $\hat{f}_j = \left(f_{j\uparrow} f^+_{j\downarrow} f_{j\downarrow} f^+_{j\uparrow}\right)^T$, where $f_{j\sigma}$ is the annihilation operator of an electron with the spin projection σ at the jth site of the NW or SW [29]. Then, we can specify the matrix Green's function of the ring in the form

$$\hat{G}^{ab}(\tau, \tau') = -i\left\langle T_C \hat{\Psi}(\tau_a) \otimes \hat{\Psi}^+(\tau'_b)\right\rangle, \quad (5)$$

where T_C is the ordering operator at the Keldysh time contour consisting of the lower (superscript +) and upper (superscript −) parts [30]; $a, b = +,-$; and $\hat{\Psi}$ has the dimension $4(N + 4n)\times 1$; i.e., it includes the Nambu operators for both SW and all NWs,

$$\hat{\Psi} = \left(\hat{b}_{L1}...\hat{b}_{Ln}\hat{d}_{L1}...\hat{d}_{Ln}\hat{a}_1...\hat{a}_N\hat{b}_{R1}...\hat{b}_{Rn}\hat{d}_{R1}...\hat{d}_{Rn}\right)^T. \quad (6)$$

The electron current in the left contact is written as $I = e\left\langle \dot{N}_L \right\rangle$ ($N_L = \sum_{k\sigma} c^+_{Lk\sigma} c_{Lk\sigma}$ is the particle number operator in the left contact). The solution of the Heisenberg equation gives ($\hbar = 1$)

$$I = 2e\sum_k \mathrm{Tr}\Big[\hat{\sigma}\mathrm{Re}\{\hat{t}^+_1(t)\hat{G}^{+-}_{k,L1}(t,t) + \hat{t}^{\,+}_n(t)\hat{G}^{+-}_{k,Ln}(t,t)\}\Big]. \quad (7)$$

Here, $\hat{\sigma} = \mathrm{diag}(1,-1,1,-1)$,

$$\hat{t}_{1,n} = \frac{t_{1,2}}{2}\mathrm{diag}\left(e^{-i\frac{eVt}{2}}, e^{i\frac{eVt}{2}}, e^{-i\frac{eVt}{2}}, e^{i\frac{eVt}{2}}\right)\hat{\sigma} \quad (8)$$

are the diagonal matrices that depend on the time and result from the unitary transformation [31] converting the voltage dependence into the operator $\hat{V}$, and $\hat{G}^{+-}_{k,L1} = i\left\langle \hat{b}^+_{L1} \otimes \hat{c}_{Lk}\right\rangle$ and $\hat{G}^{+-}_{k,Ln} = i\left\langle \hat{d}^+_{Ln} \otimes \hat{c}_{Lk}\right\rangle$ are the mixed Green's functions. In the Nambu operator space, $\hat{H}_D$ has the form of the Hamiltonian for free particles; therefore, in specifying averages in $\hat{G}^{+-}_{k,L1}$ and $\hat{G}^{+-}_{k,Ln}$, we should use the same guidelines as those for the averages for the T_C-ordered product of the second quantization operators [32, 33]. As a result, at $t \to 0$, Eq. (7) is transformed to

$$I = 2e\int_C d\tau_1 \mathrm{Tr}\Big[\hat{\sigma}\mathrm{Re}\Big\{\hat{\Sigma}^{+a}_{L1,L1}(-\tau_1)\hat{G}^{a-}_{L1,L1}(\tau_1) + \hat{\Sigma}^{+a}_{Ln,Ln}(-\tau_1)\hat{G}^{a-}_{Ln,Ln}(\tau_1) + \hat{\Sigma}^{+a}_{L1,Ln}(-\tau_1)\hat{G}^{a-}_{Ln,L1}(\tau_1) + \hat{\Sigma}^{+a}_{Ln,L1}(-\tau_1)\hat{G}^{a-}_{L1,Ln}(\tau_1)\Big\}\Big], \quad (9)$$

where $\hat{\Sigma}^{+a}_{Li,Lj}(-\tau_1) = \hat{t}^+_i(0)\hat{g}^{+a}_{Lk}(-\tau_1)\hat{t}_j(\tau_1)$ are the self-energies of the left contact ($i, j = 1, n$); $\hat{g}^{+a}_{Lk}(-\tau_1)$ is the bare Green's function of the left contact. Integrating over the time τ_1 and using the Fourier transform, we get

$$I = e\sum_{i,j=1,n}\int_{-\infty}^{+\infty}\frac{d\omega}{\pi}\mathrm{Tr}\Big[\hat{\sigma}\mathrm{Re}\Big\{\hat{\Sigma}^r_{Li,Lj}(\omega)\hat{G}^{+-}_{Lj,Li}(\omega) + \hat{\Sigma}^{+-}_{Li,Lj}(\omega)\hat{G}^a_{Lj,Li}(\omega)\Big]\Big\}. \quad (10)$$

The further transformation of Eq. (10) makes it possible to obtain an explicit form of the components associated with the local Andreev reflection and the nonlocal transfer of charge carriers. However, these lengthy expressions are not presented here.

Since many-particle interactions are absent in the system, the Green's functions in Eq. (10) are determined taking into account all the tunneling processes between the device and contacts [33]. In particular, block matrices $\hat{G}^a_{Lj,Li}$ of the advanced Green's function of the whole device $\hat{G}^a$ are determined by the Dyson equation

$$\hat{G}^a = \left[\left(\omega - \hat{h}_D - \hat{\Sigma}^r(\omega)\right)^{-1}\right]^+, \quad (11)$$

where $\hat{\Sigma}^r(\omega)$ is the retarded self-energy matrix describing the effect of both contacts on the ring. In the further numerical calculations, we will use the popular approximation of wide-band contacts, for which the real parts of the self-energy functions can be neglected and the imaginary parts can be considered as constants (see, e.g., [34]). Then, we have the following nonzero blocks of $\hat{\Sigma}^r$:

$$\hat{\Sigma}^r_{L1,L1} = \hat{\Sigma}^r_{Rn,Rn} = -\frac{i}{2}\hat{\Gamma}_{11}, \hat{\Sigma}^r_{R1,R1} = \hat{\Sigma}^r_{Ln,Ln} = -\frac{i}{2}\hat{\Gamma}_{22}, \quad \hat{\Sigma}^r_{L1,Ln} = \hat{\Sigma}^r_{R1,Rn} = \hat{\Sigma}^r_{Ln,L1} = \hat{\Sigma}^r_{Rn,R1} = -\frac{i}{2}\hat{\Gamma}_{12}. \quad (12)$$

Here, $\Gamma_{12} = \sqrt{\Gamma_{11}\Gamma_{22}}$ and $\hat{\Gamma}_{ii} = \Gamma_{ii}\hat{I}_4$, i = 1, 2, where $\Gamma_{ii} = 2\pi t_i^2\rho$ are the functions characterizing the broadening of energy levels of the device caused by its interaction with the contact, $\hat{I}_4$ is the 4×4 identity matrix, and ρ is the density of states in the contact. Consider-

ing directly the asymmetric (symmetric) ring, we assume that $\Gamma_{22} = \Gamma_{11}/2 = 0.01$ ($\Gamma_{22} = \Gamma_{11} = 0.01$).

The blocks $\hat{G}^{+-}_{\mathrm{L}i,\mathrm{L}j}$ in Eq. (10) are obtained by the solution of the Keldysh equation, $\hat{G}^{+-} = \hat{G}^{\mathrm{r}}\hat{\Sigma}^{+-}\hat{G}^{\mathrm{a}}$. Note that we consider the regime where all the transient processes have ended and the bare Green's functions of the device are not involved in this equation [33]. Here, nonzero blocks $\hat{\Sigma}^{+-}$ are given by the expressions

$$\hat{\Sigma}^{+-}_{\alpha i,\alpha j} = -2\hat{\Sigma}^{\mathrm{r}}_{\alpha i,\alpha j}\hat{F}_{\alpha}, \quad \alpha = \mathrm{L},\mathrm{R}, \quad i,j = 1,n,$$

$$\hat{F}_{\mathrm{L(R)}} = \mathrm{diag}\big(n(\omega \pm eV/2), \quad n(\omega \mp eV/2), \quad n(\omega \pm eV/2), \quad n(\omega \mp eV/2)\big), \tag{13}$$

where $n(\omega \pm eV/2)$ are the Fermi–Dirac functions.

3. We now present the results of the numerical calculation of quantum transport in the regime of linear response and low temperatures ($eV, k_{\mathrm{B}}T \approx 0$) for the system shown in Fig. 1. First, we consider the limiting case of a ring with a minimum number of sites, $n = 1$, $N = 2$. In Fig. 2a, we show the dependence of the energies of the first four states, E_{1-4}, on the gate field energy. At $h, \alpha = 0$, the energies are pairwise degenerate (see thin dotted curves). In addition, since the superconducting pairing in the ring is inhomogeneous, the gap arises at $\epsilon_d \neq 0$. However, at zero gate field, $E_{1-4} = 0$ and, hence, the conductance, $G = dI/dV$, exhibits resonance only at $\epsilon_d = 0$ (see the dotted line in Fig. 2b).

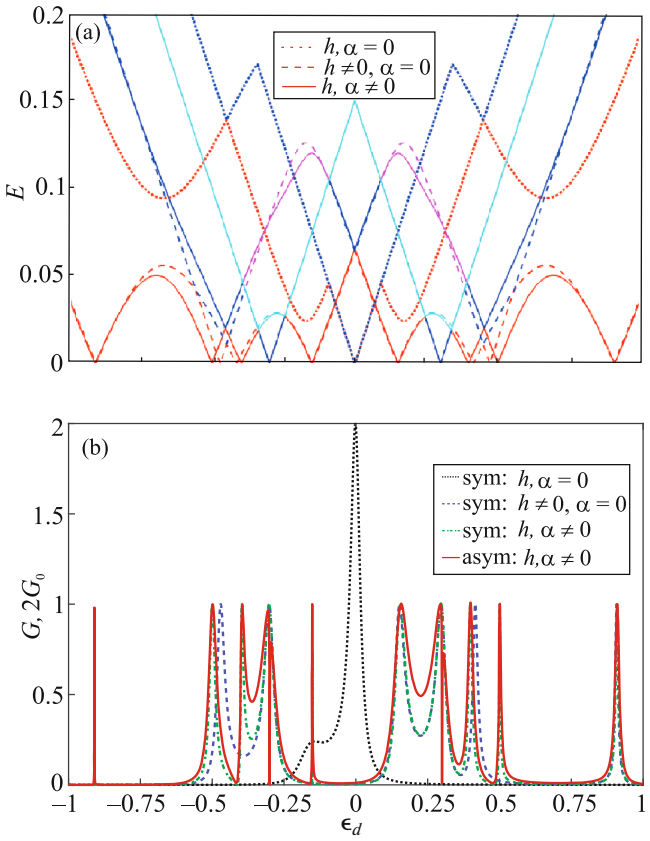

Fig. 2. (Color online) (a) Excitation energies E_{1-4} and (b) conductance of the ring consisting of six sites versus electric field energy in the gate. The parameters are $n = 1$, $N = 2$, $t_0 = 0.5$, and $h = 0.3$.

At $h > \Delta$, the gap is suppressed and the number of zeros in the spectrum becomes doubled because of the Zeeman splitting (see the dashed lines in Fig. 2a). As a result, the number of conductance peaks increases; this is illustrated by the dashed curve in Fig. 2b. However, not all zeros in the excitation energies manifest themselves as resonances in the conductance, which is a signature of arising BSCs [7, 10]. There are several ways to achieve a finite value of their lifetime. For example, the spatial symmetry of the eigenstates in the ring can be broken by introducing the spin–orbit coupling [35]. As a result, the zeros of the excitation spectrum associated with the SW are slightly shifted, and Fano resonances arise in the conductance (see the solid and dash-dotted curves in Figs. 2a and 2b, respectively). Thus, to have the Dicke effect in a symmetric ring with the superconducting central region, we need the combined effect of the magnetic field and spin–orbit coupling.

Note that the zero-energy state at $\epsilon_d = \pm h$ remains doubly degenerate even at $\alpha \neq 0$. Such degeneracy is also due to the symmetry of the ring under study and implies the existence of additional BSCs [36, 37]. Their existence can manifest itself in the conductance if we introduce the asymmetry of the tunneling parameters to the contacts. The solid curve in Fig. 2b shows that additional Fano resonances appear in this case at $\epsilon_d = \pm h$. A similar effect arises if the Aharonov–Bohm phase is taken into account [9, 10].

If the NWs and SW in the ring contain a larger number of sites, $N = 30$ and $n = 20$, respectively, the Dicke effect also takes place under the condition (2) and at $\alpha \neq 0$ [29]. This regime means the implementation of a topologically nontrivial phase in the SW. The solid curve in Fig. 3a denotes a pair of resonances, Fano and Breit–Wigner ones, in the conductance of a symmetric ring ($N = 30$ and $n = 20$) as a function of Zeeman energy. As mentioned above, the properties of the Fano resonance in this case depend on the degree of localization of the MS, which makes it possible to use such device for the detection of these excitations.

Additional features in the electron transport related to the nonlocality of the MS occur in an asymmetric ring. In this case, an additional narrow Fano resonance arises near the wide antiresonance (see the dashed curve in Fig. 3a). It is important to note that, with the increase in the bridge length, the wide

antiresonance approaches the narrow Fano peak. In turn, the latter collapses, which is clearly seen in Fig. 3b, and the BSC appears. In other words, this can be interpreted as a peculiar topological blockade of the Fano effect, associated with the asymmetry of the transport processes in the ring, since the corresponding resonance disappears just because of the nonlocality of the low-energy excitation in the SW.

To understand the mechanism underlying the collapse of the Fano resonance, it is important to recall that this resonance is determined by the BSC arising because of the degeneracy of the eigenstates of a closed system with zero energy. Hence, the disappearance of the Fano resonance could suggest an increase in the multiplicity of the degeneracy of this state if the overlap of the Majorana wavefunctions becomes negligible. To test this hypothesis, we consider the spinless model of the ring with $n = 1$. In this situation, we use the Kitaev chain with an even number of sites in the bridge [24]. Then, the Hamiltonian of the ring at $\varepsilon_d = \mu = 0$ has the form

$$H_D = \sum_{j=1}^{N-1}(-ta_j^+a_{j+1} + \Delta a_j^+a_{j+1}^+) - t_0a_1^+(b_{Ln} + b_{Rn}) - t_0a_N^+(d_{L1} + d_{R1}) + \text{H.c.} \quad (14)$$

The diagonalization of Hamiltonian (14) leads to the following equation for the excitation spectrum:

$$E^4\left(EP_1 - 2t_0^2\delta_1^{N/2-1}\right)\left(EP_2 + 2t_0^2\delta_1^{N/2-1}\right) \times \left(EP_3 - 2t_0^2\delta_2^{N/2-1}\right)\left(EP_4 + 2t_0^2\delta_2^{N/2-1}\right) = 0, \quad (15)$$

where $\delta_{1,2} = t \mp \Delta$ and P_i, $i = 1{-}4$, are the polynomials of power $N/2$ with the property $P_{2,4} = P_{1,3}(E \to -E)$ caused by the electron–hole symmetry. It follows from (15) that, for the special case of the Kitaev model, $\Delta = \pm t$, where the wavefunctions of the Majorana fermions do not overlap, the multiplicity of the degeneracy for the zero-energy state increases at $N > 2$. This is just the reason for the suppression of the narrow Fano resonance illustrated in Fig. 3b.

To make the situation clearer, we consider this system in the Majorana representation, $a_j = (\gamma_{1j} + i\gamma_{2j})/2$, where $\gamma_{ij} = \gamma_{ij}^+$ $(i = 1, 2)$. In Figs. 4a and 4b, we schematically present the device in the framework of such description for the special case of the Kitaev model, $\Delta = t$, for $N = 2$ and $N > 2$, respectively (straight lines denote the interaction between Majorana fermions of different kinds). We can see that the upper and lower arms in the former case remain connected because of the absence of superconducting pairing in horizontal directions. In the latter case, the device is divided into upper and lower identical subsystems. Each of them includes two chains of interacting quasiparticles. The self-energies of a chain with only

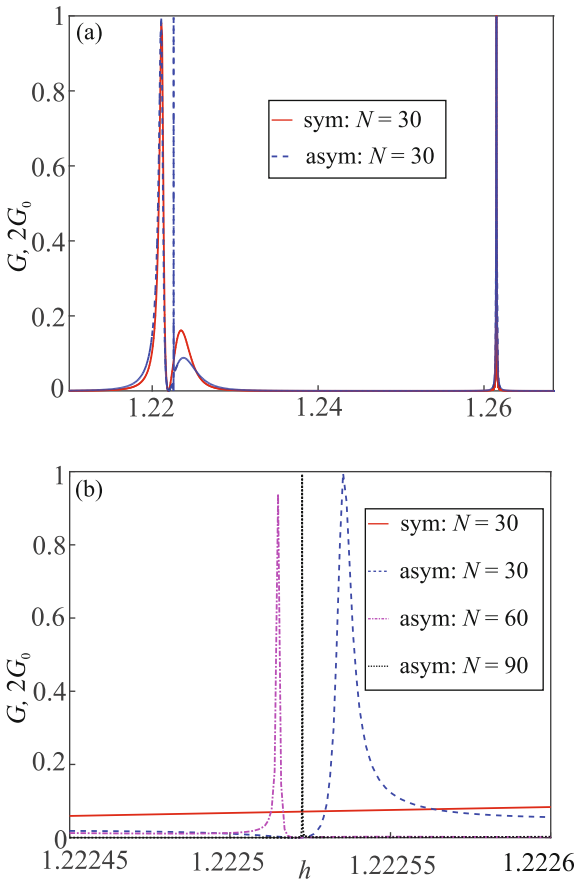

Fig. 3. (Color online) (a) Fano resonance caused by the asymmetry of the tunneling processes in the ring. (b) Collapse of the Fano resonance illustrated in panel (a) with the increase in the degree of MS nonlocality. The parameters are $n = 20$, $N = 30$, $t_0 = 0.1$, and $\epsilon_d = 1$.

two bonds in the horizontal direction are $E_1 = 0$ and $E_{2,3} = \pm t_0/\sqrt{2}$. If the vertical bond is included (in much the same way as the Fano–Anderson model), $E_{1,2} = 0$ and $E_{3,4} = \pm\sqrt{t^2 + t_0^2/2}$. Thus, it is the formation of the T-shaped structures of Majorana fermions that leads to the suppression of the Fano resonance in the asymmetric ring. Note that the nonlocality of the MS does not depend on the ratio of the tunneling parameters between the subsystems (contacts, NW, and SW); therefore, the effect under discussion has a universal nature and arises in the most general situation typical of experiment, namely, when all these parameters are different. In addition, according to Fig. 4, it is clear that the Fano resonance is not suppressed at $t = 0$, i.e., in the case of two noninteracting arms. We should emphasize that the described Fano resonance in the symmetric case does not arise in principle.

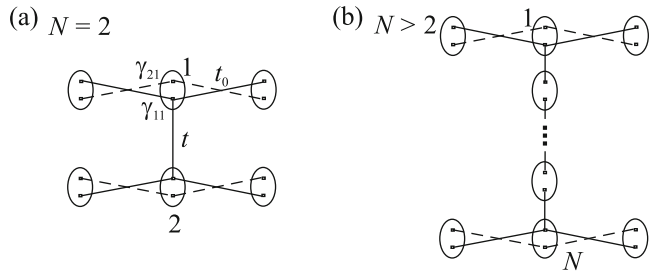

Fig. 4. Ring with $n = 1$ in the representation of Majorana operators at (a) $N = 2$ and (b) $N > 2$ for $\Delta = t$.

4. To summarize, we have analyzed the characteristic features of low-energy quantum transport related to the asymmetry of kinetic processes in the Aharonov–Bohm ring whose arms are connected by a superconducting wire in a topologically nontrivial phase. It has been found that the Fano resonance arising because of such symmetry breaking collapses with an increase in the bridge length or, in other words, when the overlap of the Majorana wavefunctions becomes negligible. To explain this effect, we have considered the model of a spinless ring, where the Kitaev chain acts as the superconducting wire. The analytical calculation of the spectrum of such system reveals an increase in the multiplicity of the degeneracy of the zero-energy state for the special case of the Kitaev model at $N > 2$ because of the formation of the T-shaped chains of Majorana fermions. This is a direct consequence of the nonlocality of the MS.

ACKNOWLEDGMENTS

We are grateful to V.V. Valkov and A.D. Fedoseev for stimulating discussions.

FUNDING

The work was supported by the Presidium of the Russian Academy of Sciences (Program of Basic Research no. 32 "Nanostructures: Physics, Chemistry, Biology, and Fundamentals of Technologies"), by the Russian Foundation for Basic Research (project nos. 19-02-00348, 20-32-70059, and 20-02-00015), and by the Government of the Krasnoyarsk Territory together with the Krasnoyarsk Science Foundation (project no. 19-42-240011 "Coulomb Interactions in the Problem of Majorana Modes in Low-Dimensional Systems with Nontrivial Topology"). S.V. Aksenov acknowledges the support of the Council of the President of the Russian Federation for Support of Young Russian Scientists and Leading Scientific Schools, grant no. MK-3722.2018.2. M.Yu. Kagan acknowledges the support of the National Research University Higher School of Economics (program of basic research).

REFERENCES

1. J. von Neumann and E. Wigner, Phys. Z **30**, 465 (1929).
2. C. W. Hsu, B. Zhen, A. Douglas Stone, J. D. Joannopoulos, and M. Soljacic, Nat. Rev. Mater. **1**, 16048 (2016).
3. R. L. Schult, D. G. Ravenhall, and H. W. Wyld, Phys. Rev. B **39**, 5476 (1989).
4. H. Friedrich and D. Wintgen, Phys. Rev. A **32**, 3231 (1985).
5. J. M. Foley, S. M. Young, and J. D. Phillips, Phys. Rev. B **89**, 165111 (2014).
6. M. Yu. Kagan and S. V. Aksenov, JETP Lett. **107**, 493 (2018).
7. M. L. Ladron de Guevara, F. Claro, and P. A. Orellana, Phys. Rev. B **67**, 195335 (2003).
8. U. Fano, Phys. Rev. **124**, 1866 (1961).
9. P. A. Orellana, M. L. Ladron de Guevara, and F. Claro, Phys. Rev. B **70**, 233315 (2004).
10. H. Lu, R. Lu, and B.-F. Zhu, Phys. Rev. B **71**, 235320 (2005).
11. R. H. Dicke, Phys. Rev. **89**, 472 (1953).
12. C. S. Kim and A. M. Satanin, J. Exp. Theor. Phys. **88**, 118 (1999).
13. C. S. Kim, A. M. Satanin, Y. S. Joe, and R. M. Cosby, J. Exp. Theor. Phys. **89**, 144 (1999).
14. W. Gong, Y. Han, and G. Wei, J. Phys.: Condens. Matter **21**, 175801 (2009).
15. A. F. Sadreev and T. V. Babushkina, JETP Lett. **88**, 360 (2008).
16. M. Yu. Kagan, V. V. Val'kov, and S. V. Aksenov, Phys. Rev. B **95**, 035411 (2017).
17. M. L. Vallejo, M. L. Ladron de Guevara, and P. A. Orellana, Phys. Lett. A **374**, 4928 (2010).
18. M. Yu. Kagan, V. V. Val'kov, and S. V. Aksenov, J. Magn. Magn. Mater. **440**, 15 (2017).
19. H.-W. Lee, Phys. Rev. Lett. **82**, 2358 (1999).
20. A. F. Sadreev and I. Rotter, J. Phys. A: Math. Gen. **36**, 11413 (2003).
21. R. M. Lutchyn, J. D. Sau, and S. Das Sarma, Phys. Rev. Lett. **105**, 077001 (2010).
22. Y. Oreg, G. Refael, and F. von Oppen, Phys. Rev. Lett. **105**, 177002 (2010).
23. V. V. Val'kov, V. A. Mitskan, A. O. Zlotnikov, M. S. Shustin, and S. V. Aksenov, JETP Lett. **110**, 140 (2019).
24. A. Yu. Kitaev, Phys. Usp. **44**, 131 (2001).
25. V. Mourik, K. Zuo, S. M. Frolov, S. R. Plissard, E. P. A. M. Bakkers, and L. P. Kouwenhoven, Science (Washington, DC, U. S.) **336**, 1003 (2012).
26. H. Zhang, C.-X. Liu, S. Gazibegovic, et al., Nature (London, U.K.) **556**, 74 (2018).
27. C.-X. Liu, J. D. Sau, T. D. Stanescu, and S. Das Sarma, Phys. Rev. B **96**, 075161 (2017).

28. V. V. Val'kov, V. A. Mitskan, and M. S. Shustin, JETP Lett. **106**, 798 (2017).

29. V. V. Val'kov, M. Yu. Kagan, and S. V. Aksenov, J. Phys.: Condens. Matter **31**, 225301 (2019).

30. L. V. Keldysh, Sov. Phys. JETP **20**, 1018 (1964).

31. D. Rogovin and D. J. Scalapino, Ann. Phys. (N. Y.) **86**, 1 (1974).

32. S. V. Vonsovskii, Yu. A. Izyumov, and E. Z. Kurmaev, *Superconductivity of Transition Metals: Their Alloys and Compounds* (Nauka, Moscow, 1977; Springer, Berlin, New York, 1982).

33. P. I. Arseev, Phys. Usp. **58**, 1159 (2015).

34. P. I. Arseev, N. S. Maslova, and V. N. Mantsevich, J. Exp. Theor. Phys. **115**, 141 (2012).

35. M. P. Nowak, B. Szafran, and F. M. Peeters, Phys. Rev. B **84**, 235319 (2011).

36. A. Volya and V. Zelevinsky, Phys. Rev. C **67**, 054322 (2003).

37. A. F. Sadreev, E. N. Bulgakov, and I. Rotter, Phys. Rev. B **73**, 235342 (2006).

Translated by K. Kugel